Analysis of Inadvertent Microprocessor Lag Time on Eddy Covariance Results

KARL ZELLER,* GARY ZIMMERMAN,+ TED HEHN,# EVGENY DONEV,@
DIANE DENNY,& AND JEFF WELKER#

* *U.S. Department of Agriculture Forest Service, Fort Collins, Colorado*
+ *Applied Technologies, Inc., Longmont, Colorado*
# *Department of Renewable Resources, University of Wyoming, Laramie, Wyoming*
@ *Department of Meteorology, Sofia University, Sofia, Bulgaria*
& *Mathematics Department, University of Wyoming, Laramie, Wyoming*

(Manuscript received 1 May 2000, in final form 1 December 2000)

ABSTRACT

Researchers using the eddy covariance approach to measuring trace gas fluxes are often hoping to measure carbon dioxide and energy fluxes for ecosystem intercomparisons. This paper demonstrates a systematic microprocessor-caused lag of −0.1 to −0.2 s in a commercial sonic anemometer–analog-to-digital datapacker system operated at 10 Hz. The result of the inadvertent negative lag (i.e., the digitized analog concentration signal is received *before* its corresponding instantaneous wind and temperature signal) is a loss in the magnitude of the recorded measured flux. Based on raw field data specific to the system used in this study (2.6-m sample height; roughness length = 3 cm), errors in flux measurements due to a 0.2-s lag ranged from 10% to 31%. Theoretical flux errors, based on ideal near-neutral cospectra, for a 0.2-s phase shift range from 21% to 55% for neutral-stability wind speeds of 0.5–15 m s^{-1}. The application of a 0.2-s phase correction improved an early-summer, sage shrubland ecosystem energy balance by 29.5%. Correction equations for lag times of 0.1–0.4 s at the sample height of 2.6 m are provided.

1. Introduction

Research in micrometeorology and ecosystem physiology has increasingly relied upon the eddy covariance technique for helping to quantify both trace-gas canopy fluxes and energy component fluxes (Zeller and Nikolov 2000). Hence, many research program managers without micrometeorological expertise are employing this technique for the first time. Successful employment of the eddy covariance flux measurements requires attention to experimental detail and field validation of the system prior to data collection campaigns (Moncrieff et al. 1997). On occasion, as in the case presented here, the manufacturer specifications (or the actual hardware implementation of the stated specification) are wrongly taken for granted. Also, finalized data must incorporate known measurement (Bussinger 1986), terrain (McMillen 1988), latent and sensible heat (Leuning and Moncrieff 1990; Tanner and Greene 1980), and sensor response corrections and concerns (Moore 1986; Zeller et al. 1989; Massman et al. 1990). Equation (1) gives the essence of the eddy covariance technique for the measurement of vertical fluxes F_c, assuming flat terrain and homogeneous, stationary turbulence. Eddy deviations of atmospheric trace-gas concentrations $c' = c - \overline{c}$, sampled at rates equal to or in excess of 5 Hz (Kaimal and Finnigan 1994), are multiplied by simultaneously sampled turbulent wind eddy components u', v', and w':

$$F_c = \overline{w'(t - t_l)c'(t)}. \quad (1)$$

Here, c is the instantaneous concentration, $\overline{c}$ is an average, t is time, and t_l is the sensor (i.e., c parameter) lag time. Also, F_c can be expressed as a function of frequency n (s^{-1}), where C_{wc} is the cospectrum of the $\overline{w'c'}$ measurement:

$$F_c = \int_0^\infty C_{wc}(n)\, dn. \quad (2)$$

Trace-gas concentration measurements are made using either (or both) open-path or closed-path sensors. To obtain an accurate eddy covariance measurement, the wind and concentration eddys in Eq. (1) must be captured at the same location and moment in time. With closed-path systems, attenuation of concentration fluctuations (Massman 1991; Leuning and Judd 1996) and t_l (the lag time of the sample flow in the intake tubing) must be accounted for in processing the fluxes (Zeller et al. 1989). For open-path systems, the concentration sensor is typically placed in situ adjacent to the wind

Corresponding author address: Karl Zeller, USDA Forest Service, Rocky Mountain Research Station, 240 West Prospect St., Fort Collins, CO 80526.
E-mail: kzeller@lamar.colostate.edu

TABLE 1. List of instrumentation at the Shirley Basin sagebrush site used in this study.

Instrument or model	Height (m)	Type	Parameter	Comment
ATI 15-cm anemometer and data-packer (Jun and Sep)	2.6	Sonic anemometer	w, w'	Vertical wind
			u, u'	Horizontal wind
			v, v'	Horizontal wind
			T_v, T_v'	Virtual temperature
LI-COR 6262 (Jun and Sep)	2.6	Closed-path infrared gas analyzer	c, c'	CO_2 and H_2O concentration and fluctuation
			q, q'	
Infrared gas analyzer (Auble and Meyers, 1992; Sep only)	2.6	Open-path infrared absorption	c, c'	CO_2 and H_2O concentration and fluctuation
			q, q'	
Campbell Scientific, Inc., KH2O krypton hygrometer (Sep only)	2.6	Light adsorption	q, q'	H_2O density and fluctuation
REBS, Inc., Q*7.1	1.0	Net radiometer	R_n	
REBS, Inc., HFT-3.1	−0.1	Soil heat flux	G	

sensor; hence $t_l = 0$. Luening and Judd (1996) caution that microprocessors used in real-time eddy covariance systems may also be responsible for delaying a data signal, especially when analog signals must be digitized and meshed with digital data, as in the case presented here.

During June of 1999, carbon dioxide (CO_2) and latent and sensible heat fluxes were collected using the eddy covariance technique at 2.6 m above a sagebrush shrubland site (roughness length $z_0 = 3$ cm) in southeastern Wyoming. The CO_2 flux data are potentially useful and complete; however, the initial energy balance results indicated a problem with the eddy covariance system. Neglecting storage [H ($=\rho C_p \overline{w'\theta'}$) + LE ($=\lambda \overline{w'q'}$)], eddy-flux-measured sensible H and latent LE heat only account for 63.5% of ($R_n - G$), which is net radiation minus soil heat flux. Here θ is potential temperature, ρ is air density, q is water vapor concentration, λ is the latent heat of vaporization, and C_p is the specific heat of air at constant pressure; R_n and G were measured using traditional slow-response sensors. The less-than-desirable energy balance result is based on the regression slope [0.635 ($\pm$0.003) ($R_n - G$) + 0.0 ($\pm$33.6)], where numbers in parentheses are the regression-parameter standard errors. Eddy covariance LE values are sometimes adjusted for the damping of high-frequency fluctuations in systems with long lag times (e.g., +20% for an ~8-s lag; Goulden et al. 1996). Because our lag time was initially determined to be 0.87 s, we estimated that we were not losing much signal to eddy damping. This paper demonstrates a systematic microprocessor-caused lag of −0.1 to −0.2 s in a commercial sonic anemometer–analog-to-digital datapacker system operated at 10 Hz. The result of the inadvertent negative lag (i.e., the digitized analog concentration signal is received *before* its corresponding instantaneous wind and temperature signal) is a loss in magnitude of the recorded measured flux. Many researchers hoping to measure CO_2 fluxes for ecosystem intercomparisons use integrated eddy flux systems similar to that discussed here. With modern gigabit data storage capacity, these researchers increasingly save their ''raw'' data and run cross correlations to determine lags and maximize covariance values. Saving raw data is unfortunately not always practiced, as was the case for this study. Our purpose is to report the problem and to present the flux correction specifically for the datapacker lag problem at 2.6 m (corrections for sensor response, separation, etc., are not addressed).

2. Methods

The eddy covariance system (Zeller et al. 1989; Massman et al. 1990) was deployed at 2.6 m above a sage shrubland canopy (hereinafter called the Sage site) in the Shirley Basin, Wyoming, during June of 1999 and again in September of 1999. Additional open-path sensors were employed briefly in September to test the closed-path system as a result of the June energy balance results. Measured fluxes (Table 1 lists sensors) included CO_2, momentum, and sensible and latent heat. Standard meteorological sensors were also mounted at 3 m for routine weather measurements. The datapacker used to interface the sonic anemometer (digital output) with the other instruments (analog outputs) was the Applied Technology, Inc. (ATI), PAD 401 (Serial No. 981107). A second datapacker was also tested in September: ATI PAD 801 (Serial No. 990502). Both datapackers were programmed with ATI Data-packer, version 1.42, software.

The sample intake system consisted of a 4.5-mm inside-diameter, 2.91-m-long (sonic-to–LI-COR, Inc., system enclosure box) Teflon tube; a 5-μm Teflon filter; the LI-COR analyzer; a mass flow controller (model 840, Sierra Instruments, Inc.); an air pump (model N828KNI, KNF Neuberger, Inc.); and a 1-L dampening chamber (3.2-mm diameter) after the pump exhaust port, used to reduced pump-induced pressure fluctuations. These were plumbed in the order given. The flow rate was 6.56 L min^{-1}, thus providing barely turbulent and sometimes laminar sample flows (Reynolds numbers = 2060 $\pm$ 100).

Eddy flux data were collected at 10 Hz and processed in real time with C^{++} eddy flux software using a standard Pentium I notebook personal computer. The C^{++} program was written by T. Meyers (National Oceanic and

Atmospheric Administration/Atmospheric Turbulence and Diffusion Division) based on McMillen's (1988) original BASIC program and adapted by the University of Wyoming specifically for our Sage site and instrumental configuration. Running means were calculated using a 400-s recursive filter, and averaged flux data were output at 30-min intervals. During the June Sage experiment, data storage space was critical; hence, the 10-Hz raw data were not saved. The June sample inlet lag time t_l (tower-to–LI-COR 6262 transit time) was erroneously calculated as 0.42 s because the plumbing within the enclosure box (including the filter and the LI-COR itself) was not accounted for. In September, raw data were saved and t_l was determined to be 0.87 s based on comparisons of the LI-COR 6262 H_2O signal (closed path) with the in situ Campbell Scientific, Inc., KH2O H_2O signal (open path), which was assumed at that time to have 0.0-s lag relative to the sonic anemometer.[1] The flux program converts 0.87 s to the nearest sample time increment: 0.9 s for 10 Hz or 0.85 s for 20 Hz.

A postanalysis of the September raw data revealed a timing difference between the sonic channels (u, v, w, and virtual temperature T_v) and the open-path analog input channels. This led to an additional laboratory test of the ATI sonic–datapacker system. [Note that the sonic T_v is calculated in real time from the 3-axis wind components, hence u, v, w, and T_v results are always simultaneous within the same 0.1-s record (ATI 1998).]

To measure these timing differences, an analog voltage generator sensor (Hehn 1987) with a response time faster than the sonic anemometer response was designed and fabricated using an infrared light emitting diode (IRLED) to illuminate an infrared phototransistor (IRPT). The IRPT output was then used to produce a 500-mV response when the optical path was interrupted. This signal was then input to the ATI PAD analog-to-digital converter. The optical path of the IRLED–IRPT pair was precisely aligned with the acoustic path of the sonic anemometer. A thin opaque block, 24 cm in length, was dropped into and through the juxtaposition optic–acoustic path to provide simultaneous signals for both sonic and analog input. Response tests were performed with the datapacker set in both the ''median'' and ''average'' filtering modes (ATI 1998).

a. Datapacker–sonic system

The sonic anemometer instrument is separate from the datapacker and can provide wind and virtual temperature data independently; however, the two are also designed to operate as a system to facilitate eddy covariance measurements. The sonic is designed to output digital data. The datapacker in turn has two functions: 1) to convert analog data signals to digital and 2) to merge sonic digital data with datapacker analog-converted-to-digital data to provide a single digital data record stream consisting of all parameters. The basic internal sampling rate of a sonic anemometer and the datapacker is 5 ms or 200 Hz. The number of 5-ms samples averaged to generate an output is selectable: 20 for an output every 100 ms (10 Hz or 0.1 s) or 10 for output every 50 ms (20 Hz or 0.05 s). There are two selectable output modes for the sonic anemometer; the arithmetic mean of the 20 (or 10) samples or the median of the 20 (or 10) samples. The current datapacker version, however *always* outputs the arithmetic mean for digitized analog data (the median option is not available for analog data). The median sonic option is used to help to despike sonic data in noisy environments, and it had been used at the Sage site because it apparently provided a better (less noisy) signal. Note that the decision to use the median option at the near-ground (i.e., high-frequency turbulence) 2.6-m height is ill advised because, depending on each 20 (or 10)-data-sample distribution, it can add an additional random lag of less than 0.1 s (0.05 s). This random lag *will not show up when stored raw data are used to recalculate covariances,* because the 5-ms data are not saved.

During operation, the datapacker immediately converts each 5-ms analog input to a digital number. After 100 ms (or 50 ms) the mean datapacker values are immediately calculated and are ready for output. The sonic output, however, requires the postapplication of calibration, shadowing corrections, and so on (Kaimal and Finnigan 1994) after the completion of the 100-ms (or 50-ms) data cycle, hence a processing delay of 25 ms occurs. Table 2 provides the timing detail of the sonic–datapacker system as operated with ATI software, version 1.42 (and earlier versions). The original datapacker program design had called for an output delay, but the resulting program incorrectly implemented a 5-ms sample delay as detailed in Table 2. The 25-ms delay was mistakenly not accounted for. A review of Table 2 reveals that there are two datapacker problems: 1) a 5-ms offset between the sonic and digitized analog datapacker data used to calculate the output records and 2) the sonic output record [made up of 20 (or 10) 5-ms data points] lags the digitized analog datapacker data by one record.

b. LI-COR 6262

The LICOR 6262 also has two output options: an analyzer-provided linear digital-to-analog signal limited to 5 Hz (CO_2) and 3 Hz (H_2O) response or a nonlinear analog signal taken directly from the infrared detector (LI-COR 1996) that provides for a 10-Hz response capability. Based on the manufacturer's recommendation for eddy covariance applications, the nonlinear output option was used during this study.

[1] This lag (0.87 s vs exactly 0.8 or 0.9 s) determination resulted from an inherent C^{++} library gettime function error (Borland 1993). It does not effect our results and is not addressed in this paper.

TABLE 2. Timing relationship detail for the datapacker–sonic anemometer system.

(10 Hz) ms	(20 Hz) ms	Version-1.42 action
0	0	Datapacker triggers sonic; sonic commences sampling.
5	5	Sonic completes 1st sample and starts 2d; datapacker commences sampling (5-ms delay to account for sonic—see text).
—	—	Additional samples at 5 ms: 10 samples for 20 Hz; 20 samples for 10 Hz.
100	50	1st sonic cycle complete, raw sonic averages available; start 2d cycle; sonic commences correction calculations on 1st cycle.
105	55	1st datapacker cycle complete, commences 2d cycle and datapacker sends 1st merged record (note: 1st sonic data missing).
125	75	1st cycle sonic data transmitted to datapacker.
200	100	Datapacker triggers sonic, 2d sonic cycle complete; start 3d sonic cycle; sonic commences correction calculations on 2d cycle.
205	105	2d datapacker cycle complete, commences 3d cycle and datapacker sends 2d merged record: 1st cycle sonic + 2d datapacker.
225	125	2d cycle sonic data transmitted to datapacker.

3. Results

a. Data

At the beginning of the September field experiment, water vapor signals from both the closed-path LI-COR 6262 (digitized analog) and the open-path KH2O (digitized analog) were plotted. Individually identifiable signal shapes were used to determine the average, $t_l = 0.87$ s, value between the KH2O and LI-COR instrument water vapor output signals. This value for t_l was then used in the real-time flux software as the lag time for the air sample to traverse the inlet line from the tower to the closed-path LI-COR 6262. It was assumed (incorrectly) that the KH2O and sonic signals measured with open-path sensors would both have $t_l = 0.0$ s, given that the wind and virtual temperature signals were not evaluated at that time.

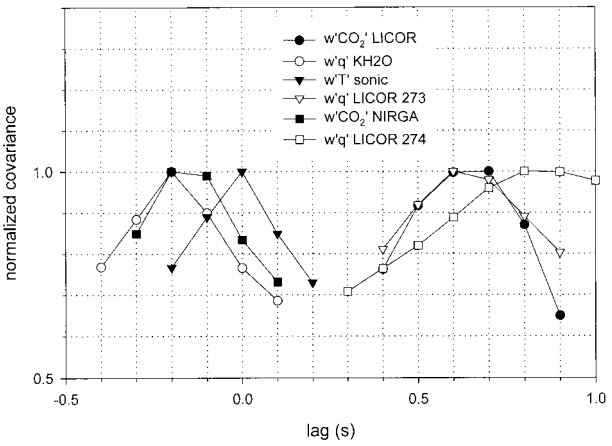

FIG. 1. Normalized eddy covariance results plotted as a function of lag time t_l for YD 273, 1200–1230 MST (also YD 274, 1200–1230 MST for LI-COR $w'q'$).

After the September field experiment, the raw field data were employed [Eq. (1)] with varying lag times to verify that $t_l = 0.87$ s (or 0.9 s, rounded up) was indeed the correct lag value for the LI-COR system. The correct lag should maximize the calculated covariance. The result (normalized examples plotted in Fig. 1) was unexpected. Additional covariance calculation tests, using data records from varied times of day and varied weather and stability conditions, provided the same results: t_l fell between 0.6 and 0.7 s for the LI-COR 6262 CO_2 output, between 0.6 and 0.85 s for the LI-COR H_2O, -0.2 s for the KH2O output, and between -0.1 and -0.2 s for the open-path infrared gas analyzer. That is, for all analog signals passing through the datapacker (10-Hz median mode), the time lag was consistently up to 0.2 s less (note minus sign for the KH2O and infrared gas analyzer results) than expected. In summary, during September data collection, the LI-COR CO_2 lag times were off by -0.2 to -0.3 s (0.9 used vs 0.6–0.7 s actual) and the LI-COR H_2O lag times were off -0.05 to -0.3 s (0.9 used vs 0.6–0.85 s actual). Except for sensible heat $\overline{w'T'}$, Table 3 presents the experimental 0.2-s correction multiplier (maximum recalculated covariance/field-measured covariance) for five sampling periods, ranging from unstable ($z/L < 0$) to stable ($z/L > 0$) atmospheric conditions, along with the average wind

TABLE 3. Eddy covariance correction 0.2-s-lag multipliers[a] for Sep 1999 test periods.

Stability (z/L)[d]	Wind (m s^{-1})	$\overline{w'q'}$ KH2O	$\overline{w'T'}$[a] if $t_l = 0.2$ s	$\overline{w'CO_2'}$ LI-COR	$\overline{w'q'}$ LI-COR	$\overline{w'CO_2'}$ open path
−1.14	2.6	1.11	1.16	1.11	1.10	—[b]
−0.11	4.3	1.23	1.36	1.37	1.12 (1.33)[c]	—
−0.06	5.3	1.30	1.38	1.31	1.23	1.20
0.012	5.2	1.32	1.44	—	1.20	1.20
1.19	1.4	—	1.18	1.25	—	—

[a] Correct lag for $\overline{w'T'}$ is 0.0 s (i.e., true multiplier is 1.0), table values are given for hypothetical event in which T' signal is 0.2 s off.
[b] Dashes indicate missing data.
[c] LI-COR $w'q'$ multiplier at 0.4-s lag, i.e., +0.8 s from w'.
[d] z = measurement height; $L = (-u_*^3 T)/(kgw'\theta')$ is Monin–Obukov length.

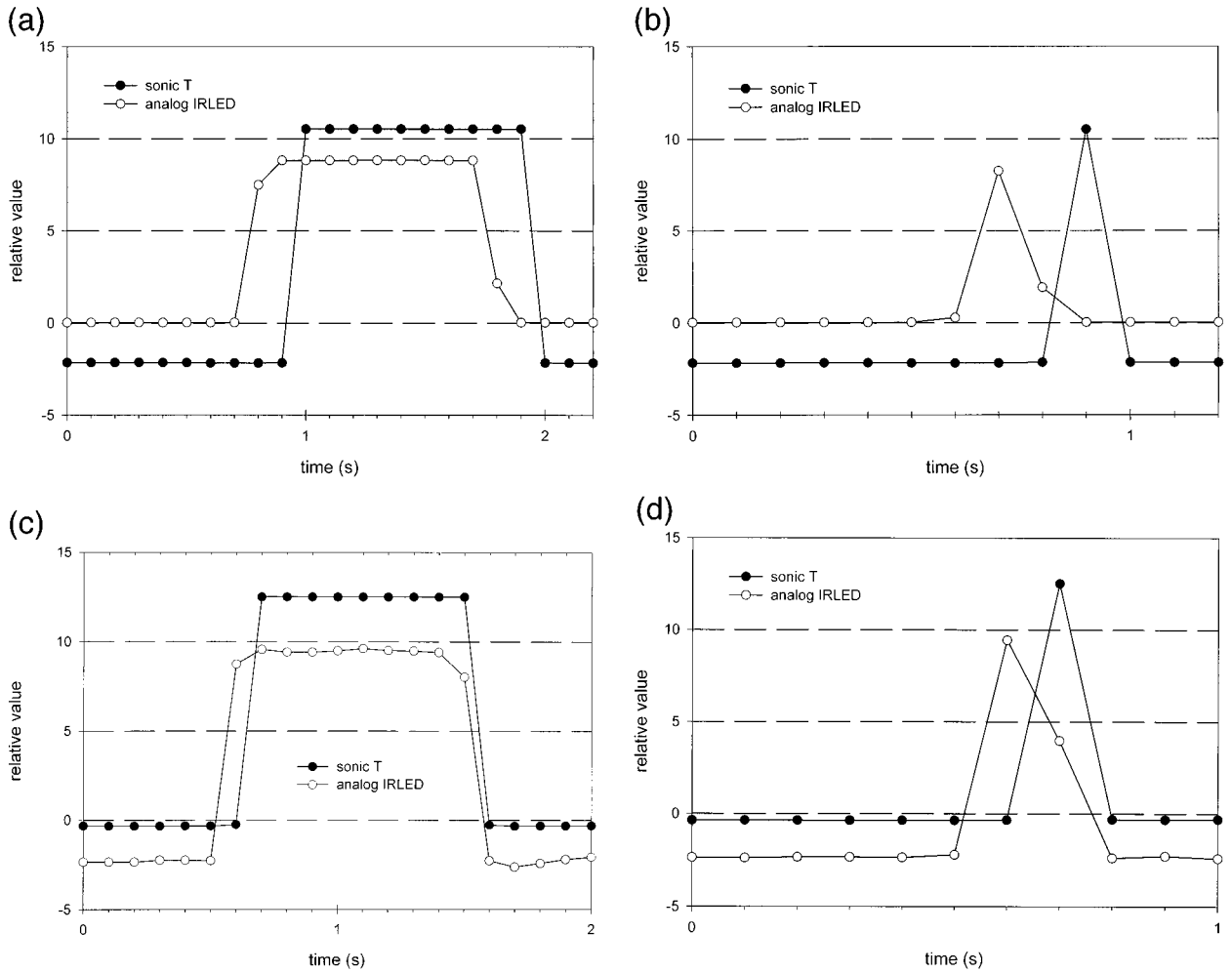

FIG. 2. Output from datapacker operating in the ''median'' mode for (a) drop, hold, and release and (b) drop through. Output from data packer operating in the ''average'' mode for (c) drop, hold, and release and (d) drop through.

speed. Here, L is the Monin–Obukov scaling length. A hypothetical sensible heat multiplier ($\overline{w'T'}$ correctly measured covariance/0.2-s lagged $\overline{w'T'}$ covariance) is included in Table 3 for comparison.

The difference in lag times between the LI-COR 6262 CO_2 and H_2O signals (Fig. 1), also noted by others (Moncrieff et al. 1997), is attributed to stickiness due to the ''electrical nature of the water vapour molecule.'' The difference in yearday (YD) 273 versus YD 274 LI-COR H_2O lag time (Fig. 1) is possibly attributed to a dirtier filter caused by a frontal passage (T dropped from 12.6° to 1°C, wind speeds increased late on YD 273, and RH increased by 50%). Mass-flow controllers also inherently sample smaller air volumes at colder temperatures, hence the increasing lag times. However, the lag increase attributed to the mass-flow-controller effect was only 3.5% (~0.02 s).

The juxtapositioned optic–acoustic path (coaligned IRLED–sonic w sensors) experiment was used to isolate and to analyze the sonic–datapacker output. The opaque block was dropped using two procedures: 1) drop to block the pathway, hold, then release to clear (Figs. 2a,c) and 2) single drop completely through the pathway (Figs. 2b,d). The results show that the sonic signals for u, v, w, and T_v consistently lagged the analog signals. There was, however, a difference between the two sonic signal output modes. Figures 2a and 2b are typical of the results for the median mode. Figure 2a (drop and block) demonstrates that the analog signal precedes the sonic signal by 0.2 s on both the blocked and cleared portions of the test. Also, the analog–digital IRLED values (Figs. 2a,b) do not reflect the actual immediate and complete step change of the test but rather an interstep average that is the result of offsetting the datapacker digitized analog data by 5 ms as compared with the sonic. It is not evident from Table 2 why there is a consistent 0.2-s lag when using the median mode. The IRLED test results were the same when repeated numerous times and when different sonic–datapacker devices were used. Figures 2c (drop and block) and 2d

TABLE 4. Equations for calculating the percent error ($100\Delta F_c/F_c$) at 2.6 m for inadvertent lag discussed in text; $\overline{u}$ = wind speed (m s^{-1}).

Lag time (s)	Height (m)	Regression equation	r^2
0.1	2.6	$1.05 + 15.99\sqrt{\overline{u}} - 1.81\ \overline{u}$	0.999
0.2	2.6	$5.26 + 24.74\sqrt{\overline{u}} - 3.09\ \overline{u}$	0.999
0.3	2.6	$9.89 + 28.61\sqrt{\overline{u}} - 3.74\ \overline{u}$	0.997
0.4	2.6	$14.24 + 30.43\sqrt{\overline{u}} - 4.10\ \overline{u}$	0.996

(drop through) for the average mode show a similar but slightly different response: 0.1-s lag on the blocked and either a 0.1- or a 0.2-s lag on the cleared portions of the test (i.e., depending on whether the IRLED data points in Figs. 2c at 1.5 s and 2d at 0.8 s are judged to be reflecting the change). It is clear, however, that the sonic average-mode inadvertent lag is shorter than the median-mode lag.

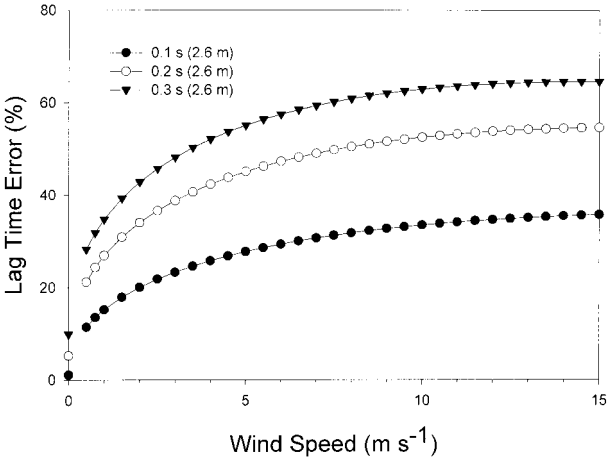

FIG. 3. Error ($100\Delta F_c/F_c$) for lag times for 0.1–0.3 s at 2.6 m vs horizontal wind speeds 0.5–15 m s^{-1}.

b. Data correction

The results given in Table 3, calculated from 10-Hz field data, demonstrate that errors in measured flux values F_m due to a 0.2-s incorrect lag time can vary at least from 10% (1.11 multiplier) to 31% (1.44 multiplier). The error attributed to such systematic lags in eddy covariance signals can theoretically be corrected using a phase-shift transfer function $T_p(n)$. From the work of Moore (1986) (Moncrieff et al. 1997; Zeller et al. 1989), the fractional underestimation or error of the measured flux ($\Delta F_c/F_c$), specifically for the signal lag in our system, would be

$$\frac{\Delta F_c}{F_c} = 1 - \frac{\int_0^n T_p(n) C_{wc}(n)\, dn}{\int_0^n C_{wc}(n)\, dn}. \qquad (3)$$

Here $\Delta F_c = F_c - F_m$ (true − measured), and $T_p(n) = \{1/[1 + (2\pi n\tau)^2]\}^{1/2}$, where τ is the lag time and we choose the sample Nyquist frequency as the upper integration limit. Table 4 provides regression expressions as percentages ($100\Delta F_c/F_c$) using the numerical results from applying Eq. (3) to theoretical near-neutral cospectra $C_{wc}(n)$, given by Kaimal et al. (1972). Eighty-one percent of the June Sage data fall within stability $-2 \le z/L \le 0.5$, valid for Kaimal's $C_{wc}(n)$ expressions. These are also plotted in Fig. 3. The error percentages are easily converted to correction multipliers: a 20% error requires a 1.25 multiplier [1/(1 − 20/100)] to correct the measured flux F_m to the desired corrected flux (i.e., $F_c = 1.25F_m$).

4. Discussion

Based on the IRLED test results, it is clear that the datapacker median analog outputs preceded the sonic by 0.2 s. Figure 4 shows the effect of applying the 0.2-s correction equation given in Table 4 to the June 1999 latent heat Sage values. The initial energy balance is improved to account for 93% of ($R_n - G$) based on the regression slope. Prior to the latent heat correction, calculated midday Sage Bowen ratios $\beta = (H/\mathrm{LE})$ ranged from 0.8 to 1.2. After the correction, midday β values dropped and ranged from 0.5 to 0.7. These latter values are more in line with unpublished $0.7 \pm 0.2\beta$ results measured in June of 1998 (YD 171–175) at the United States Department of Agriculture (USDA) Agricultural Research Service (ARS) High Plains Research Station grassland site west of Cheyenne, Wyoming (180 km southeast of the Sage site, similar climate; J. Morgan, USDA-ARS, 2000, personal communication).

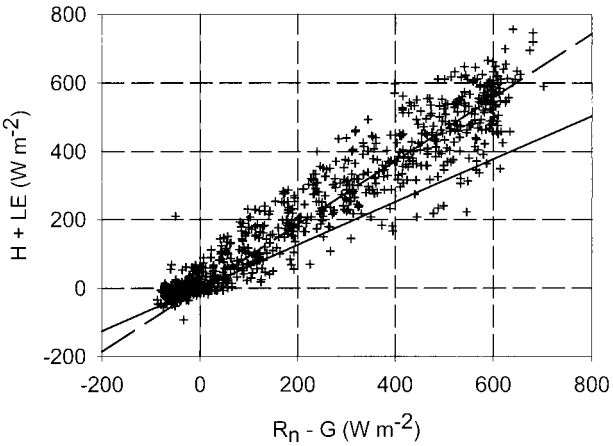

FIG. 4. Energy balance (+) after applying correction for 0.2-s lag to latent heat values. Solid line is the uncorrected regression line: (H + LE) = 0.635 (±0.003) ($R_n - G$) + 0.0 (±33.6), and dashed line is the corrected regression line: (H + LE) = 0.93 (±0.006) ($R_n - G$) + 0.0 (±60.2). Numbers in parentheses are the standard error for the regression coefficients.

5. Conclusions

Gathering accurate trace-gas eddy flux data requires careful planning, thorough system testing, and constant vigilance. An instrument problem producing a systematic 0.1-s or 0.2-s asynchronicity between the wind and trace-gas 10-Hz measurements has been shown to reduce flux estimates significantly.

The 25-ms internal datapacker processing delay at 10 Hz caused a single (0.1 s) record shift in the sonic data (u, v, w, and T_v) output when using the *average* mode and a double (0.2 s) record shift when using the *median* mode. At 20 Hz, the shifts become 0.05 and 0.1 s, respectively. Based on limited raw field data specific to the system used at the Sage site, errors in flux measurements due to a 0.2-s lag ranged from 10% to 31%. Theoretical flux measurement errors, based on ideal near-neutral cospectra, for a 0.2-s phase shift at 2.6-m, range from 21% to 55% for wind speeds of 0.5–15 m s^{-1}. The application of the 0.2-s correction improved the June 1999 energy balance by 29.5% (i.e., 93%–63.5%). Percent-error equations for lag times of 0.1–0.4 s at 2.6-m sampling height are provided in Table 4. Corrections for higher sampling heights would be smaller.

The 5-ms internal shift in real-time data acquisition between the sonic data output versus the datapacker converted-analog output was identified but not corrected for in this study. For highly responsive sensors such as open-path infrared gas analyzers employed near the ground during high-turbulence periods, applying $T_p(n)$ with a 5-ms phase shift may be a worthwhile exercise.

The manufacturer of the sonic anemometer–datapacker system evaluated here has a replacement chip (ATI version 1.5) that corrects both the 0.1–0.2-s (10-Hz mode) and the 0.05–0.1-s (20-Hz mode) lag problems.

Acknowledgments. The work presented in this paper was supported by the USDA Forest Service; the University of Wyoming; Applied Technologies, Inc.; the joint National Science Foundation and Department of Energy Program on Terrestrial Ecology and Global Change (TECO) award to the University of Wyoming. The Department of Meteorology, Sofia University, Bulgaria, provided Dr. Donev's time.

REFERENCES

ATI, 1998: Data-packer model PAD-401, operating manual. Applied Technologies, Inc., 18 pp.

Borland, 1993: Borland C^{++} version 4.0 library reference manual. Borland International, Inc., 133 pp.

Businger, J. A., 1986: Evaluation of the accuracy with which dry deposition can be measured with current micrometeorological techniques. *J. Climate Appl. Meteor.,* **25,** 1100–1124.

Goulden, M. L., J. W. Munger, S. M. Fan, B. C. Daube, and S. C. Wofsy, 1996: Measurements of carbon sequestration by long-term eddy covariance: Methods and a critical evaluation of accuracy. *Global Change Biol.,* **2,** 169–182.

Hehn, T. J., 1987: Automated data acquisition: Interfacing motion experiments to Commodore computers. B.S. thesis, Dept. of Physics, University of Northern Colorado, Greely, CO, 33 pp.

Kaimal, J. C., and J. J. Finnigan, 1994: *Atmospheric Boundary Layer Flows: Their Structure and Measurement.* Oxford University Press, 289 pp.

——, J. C. Wyngaard, Y. Izumi, and O. R. Cote, 1972: Spectral characteristics of surface layer turbulence. *Quart. J. Roy. Meteor. Soc.,* **98,** 563–589.

Leuning, R., and J. Moncrieff, 1990: Eddy-covariance CO_2 flux measurements using open- and closed-path CO_2 analyzers: Corrections for analyzer water vapour sensitivity and damping of fluctuations in air sampling tubes. *Bound.-Layer Meteor.,* **53,** 63–76.

——, and M. J. Judd, 1996: The relative merits of open- and closed-path analysers for measurement of eddy fluxes. *Global Change Biol.,* **2,** 241–253.

LI-COR, 1996: LI-6262 CO_2/H_2O Analyzer operating and service manual. LI-COR, Inc., 55 pp.

Massman, W. J. 1991: The attenuation of concentration fluctuations in turbulent-flow through a tube. *J. Geophys. Res.,* **96,** 5269–5273.

——, D. Fox, K. Zeller, and D. Lukens, 1990: Verifying eddy correlation measurements of dry deposition: A study of the energy balance components of the Pawnee Grasslands. USDA Forest Service General Research Paper RM-288, 14 pp.

McMillen, R. T., 1988: An eddy correlation technique with extended applicability to non-simple terrain. *Bound.-Layer Meteor.,* **43,** 231–245.

Moncrieff, J. B., and Coauthors, 1997: A system to measure surface fluxes of momentum, sensible heat, water vapour and carbon dioxide. *J. Hydrol.,* **188,** 589–611.

Moore, C. J., 1986: Frequency response corrections for eddy correlation systems. *Bound.-Layer Meteor.,* **37,** 17–35.

Tanner, B. D., and J. P. Greene, 1980: Measurement of sensible heat and water vapor fluxes using eddy correlation methods. Campbell Scientific Contract Rep. DAA09-87-D-0038, 17 pp.

Zeller, K. F., and N. T. Nikolov, 2000: Quantifying simultaneous fluxes of ozone, carbon dioxide and water vapor above a subalpine forest ecosystem. *Environ. Pollut.,* **107,** 1–20.

——, W. Massman, D. Stocker, D. Fox D. Stedman, and D. Hazlett, 1989: Initial results from the Pawnee eddy correlation system for dry acid deposition research. USDA Forest Service General Research Paper RM-282, 44 pp.